Biological Psychiatry

Archival Report

Intrinsic Connectivity Patterns of Task-Defined Brain Networks Allow Individual Prediction of Cognitive Symptom Dimension of Schizophrenia and Are Linked to Molecular Architecture

Ji Chen, Veronika I. Müller, Juergen Dukart, Felix Hoffstaedter, Justin T. Baker, Avram J. Holmes, Deniz Vatansever, Thomas Nickl-Jockschat, Xiaojin Liu, Birgit Derntl, Lydia Kogler, Renaud Jardri, Oliver Gruber, André Aleman, Iris E. Sommer, Simon B. Eickhoff, and Kaustubh R. Patil

ABSTRACT

BACKGROUND: Despite the marked interindividual variability in the clinical presentation of schizophrenia, the extent to which individual dimensions of psychopathology relate to the functional variability in brain networks among patients remains unclear. Here, we address this question using network-based predictive modeling of individual psychopathology along 4 data-driven symptom dimensions. Follow-up analyses assess the molecular underpinnings of predictive networks by relating them to neurotransmitter-receptor distribution patterns.

METHODS: We investigated resting-state functional magnetic resonance imaging data from 147 patients with schizophrenia recruited at 7 sites. Individual expression along negative, positive, affective, and cognitive symptom dimensions was predicted using a relevance vector machine based on functional connectivity within 17 meta-analytic task networks following repeated 10-fold cross-validation and leave-one-site-out analyses. Results were validated in an independent sample. Networks robustly predicting individual symptom dimensions were spatially correlated with density maps of 9 receptors/transporters from prior molecular imaging in healthy populations.

RESULTS: Tenfold and leave-one-site-out analyses revealed 5 predictive network-symptom associations. Connectivity within theory of mind, cognitive reappraisal, and mirror neuron networks predicted negative, positive, and affective symptom dimensions, respectively. Cognitive dimension was predicted by theory of mind and socioaffective default networks. Importantly, these predictions generalized to the independent sample. Intriguingly, these two networks were positively associated with D_1 receptor and serotonin reuptake transporter densities as well as dopamine synthesis capacity.

CONCLUSIONS: We revealed a robust association between intrinsic functional connectivity within networks for socioaffective processes and the cognitive dimension of psychopathology. By investigating the molecular architecture, this work links dopaminergic and serotonergic systems with the functional topography of brain networks underlying cognitive symptoms in schizophrenia.

https://doi.org/10.1016/j.biopsych.2020.09.024

Precise conceptualization of schizophrenia symptoms in terms of their underlying dimensional structure and associated neurobiology remains a challenge (1). Work focused on the subscales (positive, negative, and general symptoms) of the Positive and Negative Syndrome Scale (PANSS) (2) has not provided a clear understanding of underlying brain circuitry (3–5). We recently introduced a novel 4-dimensional conceptualization of schizophrenia symptomatology that is stable and generalizable across populations and settings (5). Because each symptom dimension captures a different clinical facet of schizophrenia (6–8), we would expect these to show differential relationships with functional brain networks. Identification of robust symptom-brain relationships (e.g., connectivity patterns and molecular substrates) in turn is key for developing reliable biomarkers and targeted treatments.

Previous studies proposed that abnormal brain connectivity might be a precipitating factor for schizophrenia (9,10), questioning region-based analyses but resonating with the dysconnection hypothesis (9–12). Although resting-state functional magnetic resonance imaging (fMRI) reveals broad patterns of aberrations that may underlie the pathophysiology of schizophrenia (12–15), the links between targeted symptom dimensions and associated connectivity patterns within distinct functional systems remain largely unknown. Pioneering

ISSN: 0006-3223

work has explored symptom-brain associations based on regional activity and intrinsic connectivity networks using univariate group-level correlative approaches, but the results have been largely inconsistent (16–19). The clinical complexity of schizophrenia together with the differences in patient populations, scanners, and study protocols across sites may have led to divergent results, posing a major challenge for establishing generalizable network-symptom relationships. Application of multivariable machine learning and cross-validation strategies to multisite data and validation of the resulting models on independent datasets is thus needed to derive robust network-symptom associations (20).

It needs to be cautioned, though, that intrinsic connectivity networks cannot readily be interpreted relative to cognitive and mental processes, owing to their unconstrained and task-independent nature (21). In contrast, meta-analytic functional networks are derived from task-activation data, that is, the identified networks consist of brain areas robustly engaged in specific tasks and therefore mental processes (22,23). Meta-analytic networks thus provide a promising avenue to characterize association between functionally meaningful systems and specific symptom dimensions. Considering these advantages, we performed multivariable machine learning on meta-analytically defined networks to explore predictive relationships between network-specific connectivity and dimensional psychopathology.

In order to facilitate a link to treatment, we furthermore explored whether robustly symptom-related functional networks would mirror the spatial topography of underlying molecular features, given that functional brain systems relate to molecular architecture (24–27). Specifically, connectivity-neurotransmitter coupling has been proposed and observed in healthy populations (28,29). Similarly, network dysconnectivity in schizophrenia has been associated with altered neurotransmission (30,31) involving dopaminergic, serotonergic, GABAergic (gamma-aminobutyric acidergic), and glutamatergic pathways (32–35). It is interesting to note here that current antipsychotic drugs mainly targeting the dopamine system are primarily effective against positive rather than negative or cognitive symptoms (36,37). Understanding the molecular substrate of specific dimensions of psychopathology may therefore provide leads on new treatment strategies.

We therefore assessed a broad range of meta-analytic networks relating to social, affective, executive, memory, language, and sensory-motor functions regarding their predictive power for individual positive, negative, affective, and cognitive symptom dimensions (6) in schizophrenia. Machine learning approaches with a stringent validation sequence of 10-fold cross-validation, leave-one-site-out analyses, and generalization to an independent sample was implemented to identify robust predictions. Subsequently, whole-brain density maps of 9 receptors/transporters from prior in vivo molecular imaging studies were used to investigate the molecular architecture spatially coupled to the identified predictive networks.

METHODS AND MATERIALS

Sample

A total of 147 patients with schizophrenia from 7 centers located in Europe and the United States represented the main sample (Table S1; Supplement). These sites differed significantly in illness duration ($p < .001$) (Table S1). An independent sample with 117 patients with schizophrenia (Table S2; Supplement) retrieved from the Bipolar-Schizophrenia Network on Intermediate Phenotypes (B-SNIP) database (38) was used for independent model validation. For both samples, diagnosis of schizophrenia was established based on DSM-IV, DSM-IV-TR, or ICD-10 criteria [see Supplement and (6)]. These international datasets cover a broad range of clinical states, settings, and medical systems, facilitating identification of robust network-symptom associations. Current drug dosages of antipsychotic medication were olanzapine-equivalent transformed (39). For each site, subjects gave written informed consent, and study approval was given by the respective ethics committees or institutional review boards. Approval for pooled reanalysis was provided by the ethics committee of the University of Düsseldorf, Germany.

Calculation of Dimensional Symptom Scores

Severity of psychopathology was assessed using the PANSS (2). The 30 PANSS items were compressed into 4 (negative, positive, affective, and cognitive) symptom dimensions (Figure S1A) identified in our prior factorization analysis on two large multisite schizophrenia samples as stable and well-generalizable across populations, settings, and medical systems (6). Each dimensional score for an individual was calculated as the dot product between the coefficients loaded on the particular dimension within the dimensional structure (Figure S1) and the 30 PANSS item scores of that individual (as implemented in DCTS [a dimensions and clustering tool for assessing schizophrenia symptomatology; http://webtools.inm7.de/sczDCTS/]). Higher scores on a dimension indicate more-severe symptoms (Figure S1B).

Definition of Functional Brain Networks

Seventeen functional networks, which cover a broad range of domains reflecting cognitive, socioaffective, and sensory-motor functions that have been implicated in schizophrenia, were used (Table S3). These networks were based on coordinate-based meta-analyses (21,22) and represent regions demonstrating convergent activations associated with specific functional domains across many prior task-fMRI studies. They thus provide the best a priori estimate of the location of specific functional networks and were therefore here assessed by resting-state fMRI in new subjects. For convenience, we grouped these 17 networks into 6 broad functional domains (Figure 1; Table S3), though it must be stressed that each network was analyzed separately.

fMRI Data Processing

All resting-state fMRI scans (Tables S4 and S5) were preprocessed using SPM12 (http://www.fil.ion.ucl.ac.uk/spm) [see (6) and Supplement]. After excluding subjects with excessive head motion (40) or poor image quality (see Supplement), 126 and 100 patients with schizophrenia were retained in the main and B-SNIP validation samples, respectively (Table 1). Head motion differed significantly between the sites but did not correlate with the residuals of any symptom dimensions after adjusting for age, gender, and site. Still, we adjusted head

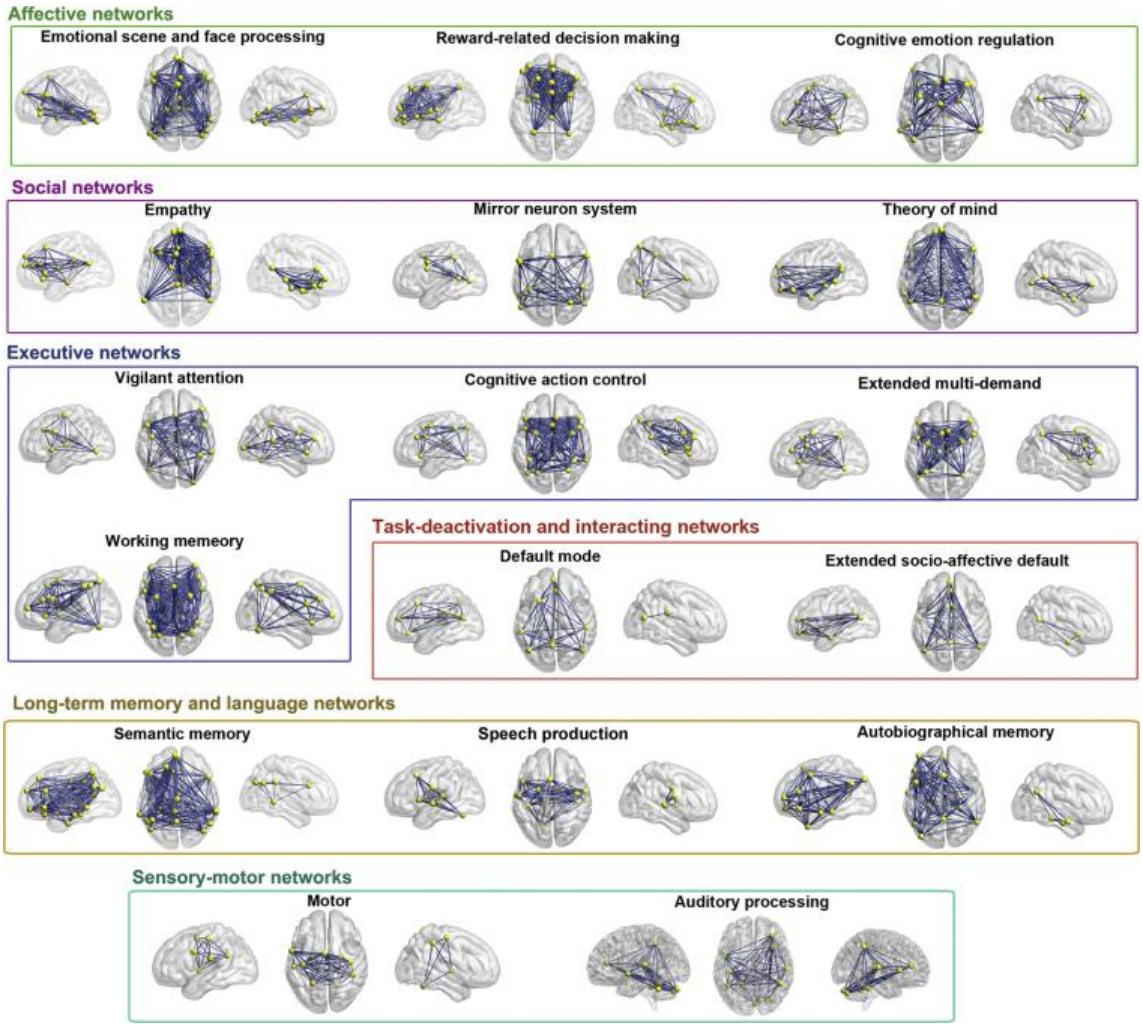

Figure 1. Overview of the 17 functional networks derived from prior coordinate-based meta-analytical studies. Networks were assigned to 6 broad domains according to their main functional roles, as implicated in the tasks included in the source publications of these meta-analytical networks, in multiple neurocognitive and socioaffective processes. We also note that networks such as the task-deactivation default mode network (22) and the extended socioaffective default network which is derived from default mode network regions (71) can be engaged during multiple processes (69,70). Details are provided in Table S3. Yellow nodes represent the spheres created from the coordinates with a 6-mm radius, and blue lines denote the pairwise connections between the nodes. Connections within each network were used separately in our predictive modeling to investigate network-specific relationships with individual dimensions of psychopathology.

motion effects in predictive modeling as a conservative approach to rule out any possible predictability based on movement.

White matter and cerebrospinal fluid signals as well as 24 head motion parameters (41,42) were regressed out from the overall fMRI time series (42), but the global mean signals were not removed given ongoing controversies (43,44). Voxels within a 6-mm sphere around each meta-analytically derived peak-activation coordinate formed a node. The first eigenvariate of the time series from all the voxels within each node was calculated as the regional characteristic time series containing better signal-to-noise ratio than the peak voxel alone. For each network, Pearson's correlation was calculated between the characteristic time series for each pair of the nodes, resulting in an $N \times N$ matrix of resting-state functional connectivity (rsFC). The upper triangle of the resulting connectivity matrix was extracted, linearized, and Fisher's Z transformed to provide the features for our predictive modeling.

Prediction of Symptom Dimensions Using Network rsFC

Multivariable regression via a relevance vector machine (RVM) (45) was implemented and evaluated using

Table 1. Demographic and Clinical Characteristics of Patients With Schizophrenia Used for Predictive Analysis

Characteristics	Main Sample (N = 126, 7 Sites)	Independent B-SNIP Sample for Validation (N = 100, 2 Sites)	p
Demographics			
Age, years	34.19 ± 11.45	34.28 ± 12.31	.948
Gender, male/female	92/34	71/29	.767
Illness duration, years	10.48 ± 9.87	12.35 ± 11.13	.187
PANSS Subscales			
Positive	14.86 ± 5.35	14.91 ± 5.72	.945
Negative	14.76 ± 5.85	15.01 ± 5.64	.743
General	30.25 ± 10.13	27.98 ± 7.46	.062
Illness severity, total PANSS	59.87 ± 18.11	57.90 ± 15.78	.390
Scores on the Dimensions of PANSS			
Negative	2.76 ± 2.44	2.81 ± 2.23	.859
Positive	3.26 ± 2.36	3.28 ± 2.55	.954
Affective	3.33 ± 2.33	2.69 ± 1.71	.022[a]
Cognitive	2.49 ± 1.92	2.72 ± 1.79	.357
Medication			
Atypical antipsychotics	97 (75.8%)	71 (71.0%)	
Typical antipsychotics	5 (3.9%)	4 (4.0%)	
Both atypical and typical antipsychotics	7 (5.5%)	13 (13.0%)	
None or unknown	19 (14.8%)	12 (12.0%)	
Current antipsychotic medication, mg/day[b]	19.23 ± 11.91	18.96 ± 13.47	

Data are presented as mean ± SD, n/n, or n (%). Except for gender, which was based on χ^2 test, other statistics were all based on 2-sample t test. Of note, because the detailed medication information was missing for several patients in different proportions for the 3 datasets, statistical comparisons were not conducted.

B-SNIP, Bipolar-Schizophrenia Network on Intermediate Phenotypes; PANSS, Positive and Negative Syndrome Scale.

[a]$p < .05$.

[b]Olanzapine-equivalent dosage.

500× repeated 10-fold cross-validation, individually for each combination of functional network and symptom dimension in the main sample. Using each network individually in the model was intended to ensure the functional specificity of our results. Importantly, RVM is a sparse learning method, that is, only a few of the learned feature weights are nonzero, lending interpretability as to which features (connections) are predictive. As recommended in (46), the symptom dimensional scores and rsFC features were adjusted for confounding effects of age, gender, site, and head motion. To avoid data leakage within cross-validation (47), confound regression models were learned only on the training set and then applied to both training and test data (48,49). The RVM model trained on the (confound-adjusted) training data and was then applied to the (confound-adjusted) held-out data. Folds were stratified to accommodate different sample sizes across sites. Prediction performance was evaluated using Pearson's correlation between the (adjusted) scores and their predictions. Significant predictions were further validated for their generalizability across sites using leave-one-site-out cross-validation following the same schematic but training on all sites but one and testing on the left-out site (Supplement). Statistical significance of the cross-validation–based correlations was determined through 1000 permutations by shuffling the symptom dimensional scores (lowest p = .001, right-tailed) (Supplement) (47,50).

Critically, we validated predictive associations confirmed by leave-one-site-out cross-validation in the independent B-SNIP sample. For this, we trained RVM models on the significantly predictive networks in the entire main sample and then, without further fitting or modification, applied them to held-out B-SNIP data. Robust associations passing this strict 3-step validation procedure were then further assessed as described below.

In addition, connections within the networks identified with robust associations with symptoms were combined to test the possible improvement in prediction performance. Control analyses were performed by repeating all validation procedures including illness duration or olanzapine-equivalent dosage as confounds. For comparison, 1) we predicted the 3 PANSS subscales (positive, negative, and general psychopathology) using the same 3-step validation procedure and each network individually as in our main analyses, and 2) we predicted the 4 symptom dimensions using the whole connectome (39,060 connections) that comprised pairwise connectivity between all the nodes pooled from the 17 meta-analytic networks.

Identification of Reliably Predictive Connections and Subnetworks

The intrinsic feature selection in RVM through its sparse modeling was leveraged to identify reliably predictive

connections and the potential subnetworks formed by them. A connection was identified as reliably predictive when it had nonzero weights in 1) at least 80% of the 10-fold cross-validation repetitions, 2) at least 6 out of the 7 (i.e., >80%) leave-one-site-out analyses, and 3) the models trained on the entire main sample for validation in B-SNIP. The cutoff of 80% is suggested as a conservative threshold in both real and simulated data (51). To assess the predictive capacity of the subnetworks, RVM models were trained using the rsFC of the subnetworks on the main sample and tested in B-SNIP.

Spatial Correlation With Receptor/Transporter Densities

Finally, we evaluated the topographical relationship between network node location and the distribution of several receptor/transporter systems, assessing for highly expressed receptors/transporters in the identified networks relative to the entire brain. This was tested by comparing the average receptor/transporter density across all nodes within a given network against a null distribution based on 1000 random network configurations generated by redistributing the nodes throughout the gray matter while preserving the between-node distances (±6 mm tolerance). Seven dopamine and serotonin receptors (dopaminergic: D_1 and D_2/D_3; serotonergic: 5-HT_{1A}, 5-HT_{1B}, and 5-HT_{2A}) and transporters (dopamine transporter and serotonin reuptake transporter [5-HTT]), together with F-DOPA (a reflection of presynaptic dopamine synthesis capacity) and the GABAergic $GABA_A$ receptor were investigated. Although all systems are linked to schizophrenia (32,34,35), we here tested specific receptors/transporters. Density estimates were derived from average group maps of healthy volunteers (D_1: n = 13; D_2/D_3: n = 7; 5-HT_{1a}: n = 35; 5-HT_{1b}: n = 23; 5-HT_{2a}: n = 19; 5-HTT: n = 18; dopamine transporter: n = 147; F-DOPA: n = 12; $GABA_A$: n = 6) scanned in prior multitracer molecular imaging studies (Supplement). For comparability, these maps, in MNI152 space, were all resampled to an isotropic 2-mm spatial resolution as in our fMRI data and linearly rescaled to 0–100.

Furthermore, the significantly higher expressed receptors/transporters were entered into a spatial correlation analysis (52,53) calculated as rank correlation between the node importance scores and receptor/transporter densities calculated for these nodes. The node importance score was calculated by summing the selection frequency of the connections of each node derived from the repeated 10-fold cross-validation. Bootstrap analysis was conducted to ensure robustness. To establish the statistical significance of a spatial correlation against chance, a spatial permutation test was used where the null distribution was estimated based on the correlations between the node importance scores for a given network and the nodal receptor/transporter densities extracted from 1000 simulated (random) networks (Supplement).

RESULTS

Network-Based Prediction of Specific Symptom Dimensions

Predictive modeling with stringent 3-step validation revealed several predictive network-psychopathology relationships. In the first step (10-fold cross-validation), the affective, negative, and positive symptom dimensions could be significantly predicted using rsFC within the mirror neuron system, theory of mind (ToM), and cognitive emotion regulation networks, respectively, while the cognitive dimension was predicted by 3 networks: ToM, empathy, and extended socioaffective default (eSAD) (Figure 2A, B). Except for the empathy-cognitive prediction, all these predictive network-symptom associations (Figure 2B) were confirmed in the second validation step, that is, the leave-one-site-out analysis (Figure 2C).

As both the 10-fold cross-validation and leave-one-site-out analyses were performed in the main sample, these analyses may still be overly optimistic regarding generalization to new patient populations. Therefore, we added a third validation step using a completely independent sample. Three of the 5 leave-one-site-out validated associations (ToM-negative, cognitive emotion regulation–positive, mirror neuron system–affective) were not confirmed in this step. However, training RVM models on the entire main sample and testing it in the B-SNIP dataset revealed that the ToM and eSAD networks were significantly predictive of cognitive symptoms (Figure 2D). Comparatively, combing the connections in these two networks yielded only a marginal improvement in the prediction of cognitive dimension in B-SNIP (r = .24, p = .018).

In complementary analyses, no significant effects of illness duration or olanzapine-equivalent dosage on the 4 symptom-dimension scores were found (all $p > .05$ in the fitted general linear models). Conversely, controlling for illness duration or olanzapine-equivalent dosage did not alter the overall predictive patterns. Highlighting the utility of our 4-dimensional conceptualization of schizophrenia symptomatology (6), predicting the traditional 3 PANSS subscales, 10-fold cross-validation and leave-one-site-out experiments on the main sample revealed only 2 predictive patterns (ToM-negative, eSAD-general psychopathology), which did not, however, generalize to B-SNIP (Figure S2). The whole-connectome comprising nodes from all networks was not predictive of any of the 4 symptom dimensions (all $r < .11$, $p > .13$; 500× repeated 10-fold cross-validation), supporting our use of individual networks as an a priori biologically meaningful dimensionality reduction.

Reliably Predictive Connections and the Predictiveness of Subnetworks

Ten connections within eSAD and 8 connections within ToM were identified as consistently relevant for predicting cognitive symptoms (Figure 3A; Table S6), that is, were selected in more than 80% of the different cross-validation runs (repeated 10-fold cross-validation and leave-one-site out) and in the final models trained on the entire main sample for validation in B-SNIP. The ensuing ToM and eSAD subnetworks featured 3 spatially overlapping nodes located in the ventromedial prefrontal cortex, left middle temporal gyrus, and posterior cingulate cortex/precuneus and highlighted the ventromedial prefrontal cortex–posterior cingulate cortex/precuneus connection (Figure 3B; Table S7). In turn, connections to subcortical regions including the bilateral amygdala/hippocampus and ventral striatum were specific to the eSAD subnetwork.

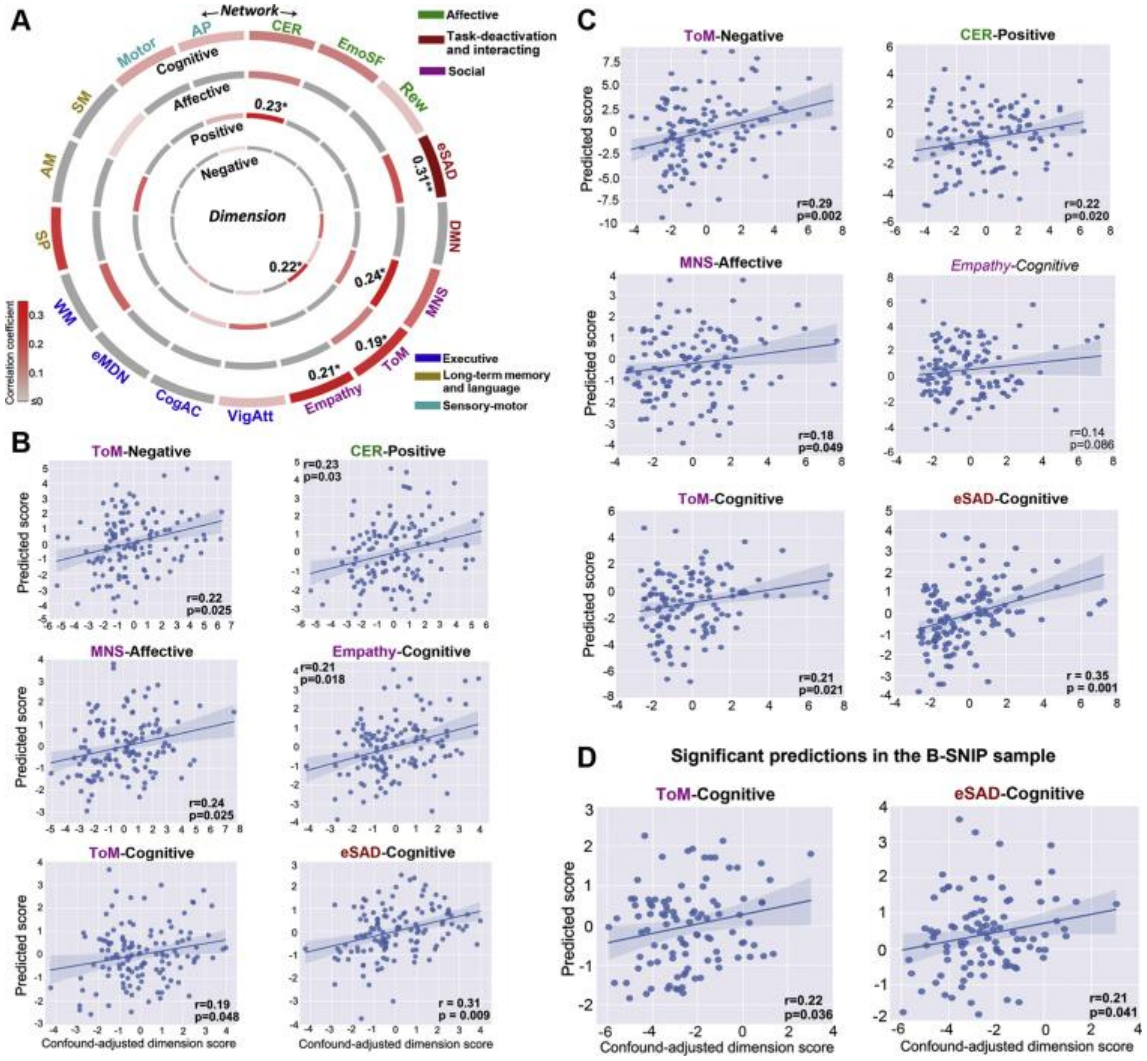

Figure 2. Multivariable prediction of the 4 symptom dimensions from within-network resting-state functional connectivity (rsFC) using relevant vector machine. **(A)** Circos plot showing the 500× repeated 10-fold cross-validation results for the main sample. Correlations between the actual (confound-adjusted) dimensional symptom scores and their predictions are color coded from light gray (0) to dark red (0.35). *$p < .05$, **$p < .01$. **(B)** Scatter plots showing the 6 significant predictions identified by 10-fold cross-validation in the main sample. **(C)** Scatter plots showing the leave-one-site-out cross-validation results for the 6 significant predictions identified by 10-fold cross-validation in the main sample. Apart from the prediction of cognitive dimension from the rsFC within the empathy network, other predictions were all confirmed by leave-one-site-out analysis with significant correlations identified. **(D)** Scatter plots showing the significant predictions in the independent Bipolar-Schizophrenia Network on Intermediate Phenotypes (B-SNIP) sample. Models trained within the main sample were used for this validation analysis in B-SNIP. Shaded areas represent 95% confidence intervals. AM, autobiographical memory; AP, auditory processing; CER, cognitive emotion regulation; CogAC, cognitive action control; DMN, default mode network; eMDN, extended multidemand network; EmoSF, emotional scene and face processing; eSAD, extended socioaffective default; MNS, mirror neuron system; Rew, reward-related decision making; SM, semantic memory; SP, speech production; ToM, theory of mind; VigAtt, vigilant attention; WM, working memory.

A model based on the identified eSAD subnetwork showed almost identical prediction performance for the B-SNIP data compared with the one trained on the whole eSAD (Figure 3C) (note that subnetwork definition was based only on the main sample, i.e., there is no leakage of information about the B-SNIP data). Interestingly, compared with the whole ToM network (Figure 2D), the ToM subnetwork demonstrated an improved performance (Figure 3C). This confirms the power of sparse modeling in RVM to identify the truly relevant features.

Relationship to Molecular Architecture

Results showed that 8 receptors/transporters (Figure 4A) are highly expressed in one or both networks (ToM, eSAD) relative

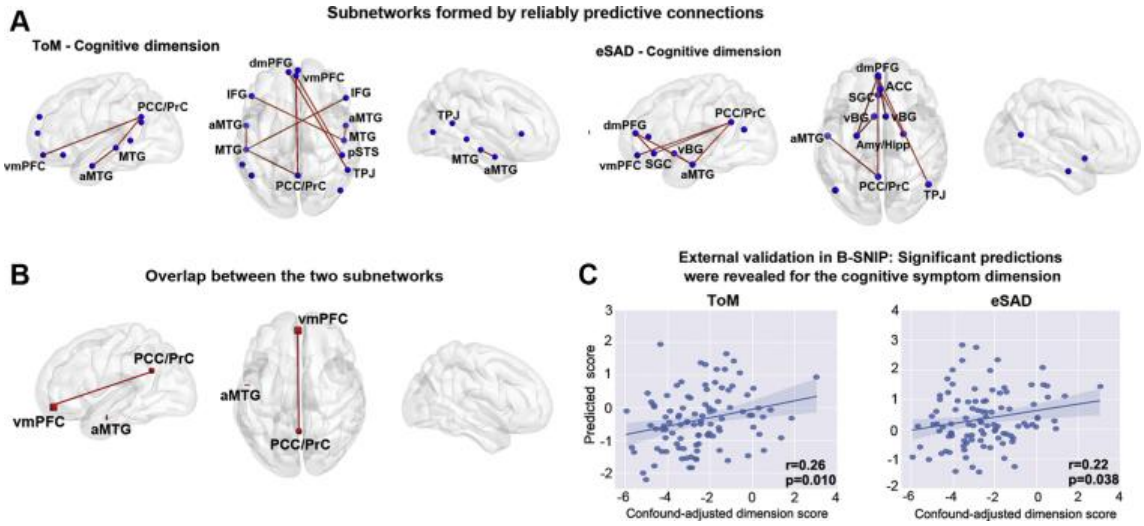

Figure 3. Reliably predictive connections for the 2 networks that robustly predicted the cognitive dimension, and validation of the formed subnetworks in the independent sample. **(A)** Reliably predictive connections selected in more than 80% of the different cross-validation runs (repeated 10-fold and leave-one-site out) and in the final models trained on the entire main sample for validation in Bipolar-Schizophrenia Network on Intermediate Phenotypes (B-SNIP). **(B)** Overlapping between the 2 subnetworks. **(C)** Scatter plots showing the significant correlations in B-SNIP using the models trained within the main sample. ACC, anterior cingulate cortex; aMTG, anterior middle temporal gyrus; Amy, amygdala; CER, cognitive emotion regulation; dmPFC, dorsomedial prefrontal cortex; eSAD, extended socioaffective default; Hipp, hippocampus; IFG, inferior frontal gyrus; mFG, medial frontal cortex; MNS, mirror neuron system; PCC, posterior cingulate cortex; PrC, precuneus; SGC, subgenual cingulate cortex; ToM, theory of mind; TPJ, temporoparietal junction; vBG, ventral basal ganglia; vmPFC, ventromedial prefrontal cortex.

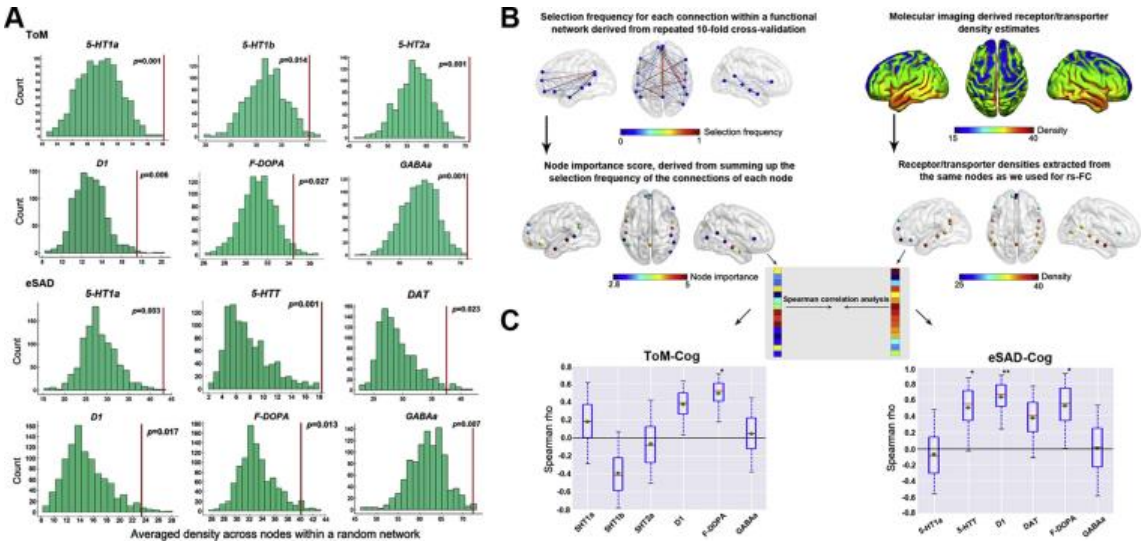

Figure 4. Significantly highly expressed receptors and transporters at the nodes of the robustly predictive networks relative to the entire brain, as well as the schematic and results for the spatial correlation analysis with receptor/transporter density maps. **(A)** Histograms showing the null distributions for the receptor/transporter densities of the 1000 simulated (random) networks. Red lines indicate the true averaged receptor/transporter densities across the different nodes within real networks. **(B)** Procedure for conducting the spatial correlation analysis between network nodes and receptor/transporter density maps. **(C)** Bootstrapped Spearman correlations (repeated 10,000 times) between the node importance score and the nodal receptor/transporter density estimates for the 2 identified networks that robustly predicted the cognitive symptom dimension. Bootstrap nodes were drawn with replacement from the real networks, and then the correlation analysis was done on them. Boxes indicate the Spearman rho values. In each box the line indicates the median, the diamond indicates the mean, and the whiskers indicate the 5th and 95th percentiles. Significant correlations derived from spatial-level permutation tests are marked with an asterisks: $^{*}p < .05$, $^{**}p < .01$. 5-HT, serotonin; 5-HTT, serotonin transporter; Cog, cognitive dimension; DAT, dopamine transporter; eSAD, extended socioaffective default; rs-FC: resting-state functional connectivity; ToM, theory of mind.

to the simulated networks with perturbed spatial configuration of nodes (histograms of node distance are shown in Figure S3). Spatial correlation between the node importance (Table S9) and the spatially corresponding density of those significant receptors/transporters (the procedure was detailed in Figure 4B) revealed a relationship to both the dopaminergic and the serotonergic systems (Figure 4C). Specifically, the nodes of ToM that showed higher importance in predicting the cognitive dimension tracked with higher dopamine synthesis capacity (r = .54, p = .02). The prediction importance of the nodes within the eSAD network correlated positively with densities of D_1 (r = .66, p = .007) and 5-HTT (r = .53, p = .046), as well as dopamine synthesis capacity (r = .54, p = .036). The significance was corroborated by bootstrapped confidence intervals.

DISCUSSION

By using predictive modeling on multisite fMRI data with a strict out-of-sample validation procedure (repeated 10-fold cross-validation, leave-one-site-out analysis, independent dataset), two a priori meta-analytically defined functional networks, ToM and eSAD, were identified as significantly and robustly predictive of the cognitive symptom dimension in patients with schizophrenia. In contrast, prediction using the original PANSS subscales failed to generalize to the independent sample, supporting the notion that these traditional dimensions do not correspond well with underlying neurobiology. Through the implicit feature selection of RVM, reliably predictive connections were identified that constituted subnetworks connecting nodes mainly distributed in the (medial) prefrontal cortex, posterior cingulate cortex, temporal regions, and subcortical structures. Moreover, higher densities of D_1 receptor and 5-HTT as well as elevated dopamine synthesis capacity were related to the node importance of the ToM and the eSAD networks in the prediction of cognitive symptomatology.

Symptom Dimensions Were Differentially Predicted by Different Functional Networks

In contrast to the prevalent notion of global or widespread brain deficits (10–12) in schizophrenia, we here revealed specific network-psychopathology relationships based on the predictive capacity of functional systems for patient-specific symptom severity along 4 dimensions. Two networks, ToM and eSAD, both predicting the cognitive dimension, passed our strict validation steps (see the Supplement and Table S8 for an additional explorative analysis correlating cognitive scores assessed using a scale other than the PANSS with the true and the predicted cognitive dimensional scores). As ToM subserves social cognition while the eSAD network relates to socioaffective processes, these results support previous findings indicating that compromised "social brain" development in schizophrenia relates to higher-level cognitive deficits (54,55). Somewhat surprisingly, these two networks did not allow a robust prediction of negative or affective symptoms, even though other socioaffective networks [cognitive emotion regulation: reappraisal process of emotional stimuli (56); mirror neuron system: emotional aspect of social cognition (18)] predicted positive and affective dimensions, respectively, in the main sample. Thus, it stands to reason that different socioaffective networks capture individual variance of different symptom dimensions. Of note, these predictions did not generalize to B-SNIP, potentially because of between-sample differences in clinical characteristics, highlighting that building models that generalize to novel cohorts remains a challenge (57). We also noted that the cognitive dimension was not robustly predicted by any of the assessed cognitive networks, mirroring previous work in healthy subjects showing that task-based functional connectivity yields better predictions of cognition than networks at rest (58–60).

In turn, intrinsic connectivity patterns within the ToM network are robustly predictive of the cognitive status in individual patients with schizophrenia. ToM is the cognitive ability of an individual to infer others' mental states, intentions, and beliefs (61). As these involve complex cognitive processes and considering that the cognitive dimension of schizophrenia psychopathology encompasses symptoms such as "conceptual disorganization," "lack of insight," and "disturbed abstract thinking," this predictive relationship is not unexpected. Conversely, ToM deficits, which are prevalent in schizophrenia and are a well-established feature and vulnerability marker of this disorder (62), are known to be associated with symptoms of disorganization (63). Abnormal neural activation in response to tasks targeting ToM also has been reported in schizophrenia, involving the temporoparietal junction as well as prefrontal and temporal regions where the current ToM meta-network is distributed (64,65).

It is interesting to note that the ToM network also predicted negative symptoms in the main sample, although this did not generalize to the B-SNIP data. Given that the subnetworks of ToM predicting negative and cognitive dimensions, respectively, were largely divergent (Figure 3B; Figure S4), this resonates with the notion that ToM encompasses multiple components (66).

Intriguingly, cognitive symptoms in schizophrenia were also linked to socioaffective processes via the prediction using the eSAD network. This corroborates recent studies consistently linking neural activity patterns in the default mode network (DMN) to cognitive abilities (67,68), and the implication of the DMN-derived eSAD network (69) in cognitive processing is therefore unsurprising. Our finding moreover resonates well with literature suggesting that socioaffective factors affect and modulate cognitive performance such as working memory and attention in patients with schizophrenia (70–72). The use of seemingly noncognitive psychosocial methods has been proposed as a potential remediation strategy for cognitive deficits in schizophrenia (70), and indeed has been successfully applied in practice (72). Consequently, we would hypothesize that the cognitive dysfunctions in schizophrenia might relate to an impaired integration of self- and other-related processes. Since the interaction of the (core) DMN with other brain regions and networks is more reflective of schizophrenia symptoms than within-DMN connectivity (18,73,74), it is not surprising that the DMN was not predictive but that the eSAD, which comprises regions going beyond the DMN, was.

Molecular Architecture of the Networks Robustly Predicted Cognitive Dimension

Cognitive deficits are a lifelong burden for patients with schizophrenia because there are so few effective medications,

including mainstay antidopaminergic agents (37,75). In line with the notion that dopaminergic dysfunction alone does not account for the whole picture of schizophrenia psychopathology (76,77), here we revealed that the networks and nodes predictive of individual cognitive symptom load are related to both dopaminergic (32) and serotonergic (76) systems. These data extend previous region-of-interest analyses (78,79) to a comprehensive topographical level and are supported by findings that cognitive deficits relate to D_1 receptor elevation in schizophrenia (78). The present extension to a network-level investigation is important, as patients with schizophrenia are characterized by dysconnection between distant brain regions, and network-based analyses can nominate mechanisms of action for the development of novel pharmacological treatments (80). In line with involvement of dopamine functioning in cognitive deficits in schizophrenia (32), the cognitive dimension of psychopathology was associated with dopamine synthesis capacity. Increased dopamine synthesis capacity in schizophrenia was reported in not only the striatum (32) but also cortical areas, including the prefrontal cortex (81,82), where multiple nodes within the ToM and eSAD networks are located.

Moreover, cognitive symptoms were linked to the density of 5-HTT, which plays a critical role in regulating serotonergic concentration and signaling. Serotonergic dysfunction and 5-HTT polymorphism (83) have been involved in schizophrenia pathophysiology (34,76). Previous postmortem and in vivo positron emission tomography studies have yielded inconsistent results on the alteration of 5-HTT density in schizophrenia (34), while an overexpression of 5-HTT messenger RNA in the prefrontal and temporal cortex has been demonstrated (84). We here revealed a potential role of 5-HTT in cognitive deficits via the networks involved in socioaffective processes, resonating with the proposed implication of 5-HTT in the affective domain (85,86). While atypical antipsychotics, including olanzapine and risperidone, also target the 5-HT_{2A} receptor (87,88), their effects on 5-HTT seem to be equivocal (89,90). Interestingly, antipsychotic drugs pimavanserin and SEP-363856 have just been introduced that preferentially target serotonin and not dopamine receptors (91,92), suggesting increased focus also on serotonergic pathways.

Limitations and Considerations

First, the effect sizes for the correlation between the symptom scores and their predictions were moderate. However, despite the clinical complexity of the population and the heterogeneities in scanners and protocols, the effect sizes are similar to those previously reported for predicting, e.g., creativity (93), personality (46), and memory performance (94) in healthy subjects (r values mostly $\sim$.2–.35). Since olanzapine-equivalent dosage did not correlate with symptom scores or alter the prediction pattern after additionally controlling for the dosage in cross-validation, medication would be largely a source of random variation in our data and thus make our results more conservative. Second, we acknowledge that task-specific changes in network topology and related dynamics may also explain the variance in individual symptoms (95,96) and should be the scope of future studies to complement our resting-state findings. Third, although meta-analytically derived peak coordinates are the most likely location of specific functional networks, there may exist individual-specific topological differences that in turn may reflect pathophysiological mechanisms underpinning individual symptoms. Future studies assessing the contribution of individual-specific topology to the prediction of symptoms are desired. Fourth, although glutamatergic dysfunction has been increasingly implicated in schizophrenia neurocognitive deficits (77,97), there are no publicly available in vivo maps reflecting the glutamatergic system. Fifth, within-subject (longitudinal) studies assessing symptoms, rsFC, and receptor densities are needed. Finally, we acknowledge that the sample sizes are modest for some of the receptor/transporter maps that we used from prior molecular imaging studies, as acquisition of molecular imaging data in large samples remains difficult.

Based on rsFC within different meta-analytic task-activation networks covering a broad range of functional domains and predictive modeling with strict validations, intrinsic connectivity patterns of networks implicated in socioaffective processing was revealed to be robustly associated with the cognitive dimension of psychopathology. Our investigation of the molecular architecture of the identified predictive networks implied a potential involvement of 5-HTT, besides the dopaminergic system, in schizophrenia cognitive symptomatology, possibly providing hints into treatments.

ACKNOWLEDGMENTS AND DISCLOSURES

This study was supported by the Deutsche Forschungsgemeinschaft (Grant No. EI 816/4-1 [to SBE]), the National Institute of Mental Health (Grant No. R01-MH074457 [to SBE]), the Helmholtz Portfolio Theme "Supercomputing and Modeling for the Human Brain" (to SBE), and the European Union's Horizon 2020 Research and Innovation Programme (Grant Nos. 785907 [HBP SGA2] [to SBE] and 945539 [HBP SGA3] [to SBE]). JC received a Ph.D. fellowship from the Chinese Scholarship Council (Grant No. CSC201609350006).

We acknowledge Laura Waite (Institute of Neuroscience and Medicine, Brain and Behaviour [INM-7], Research Center Jülich, Jülich, Germany) for proofreading.

This article was published as a preprint on bioRxiv: https://doi.org/10.1101/2020.07.02.185124.

Maps of the meta-analytic networks and the code for predictive modeling can be found at https://github.com/inm7/Network-based-prediction. Density maps of neurotransmitter receptors and transporters and the MATLAB-based toolbox for the integration of positron emission tomography– and single photon emission computed tomography–derived modalities with other brain imaging data are available at https://github.com/juryxy/JuSpace.

The authors report no biomedical financial interests or potential conflicts of interest.

ARTICLE INFORMATION

From the Institute of Neuroscience and Medicine: Brain and Behavior (INM-7) (JC, VIM, JD, FH, XL, SBE, KRP), Research Center Jülich, Jülich; Department of Psychiatry and Psychotherapy (BD, LK), Medical School, University of Tübingen, Tübingen; Institute of Systems Neuroscience (JC, VIM, JD, FH, XL, SBE, KRP), Medical Faculty, Heinrich Heine University Düsseldorf, Düsseldorf, Germany; and Section for Experimental Psychopathology and Neuroimaging (OG), Department of General Psychiatry, Heidelberg University, Heidelberg, Germany; Schizophrenia and Bipolar Disorder Program (JTB), McLean Hospital, Belmont; Department of Psychiatry (JTB), Harvard Medical School, Boston, Massachusetts; Department of Psychology (AJH), Yale University, New Haven, Connecticut; Institute of Science and Technology for Brain-Inspired Intelligence (DV), Fudan University, Shanghai, People's Republic of China; Iowa Neuroscience Institute

and Department of Psychiatry (TN-J), Carver College of Medicine, University of Iowa, Iowa City, Iowa; Université de Lille (RJ), INSERM U1172, Lille Neuroscience & Cognition Centre, Plasticity & SubjectivitY team & CHU Lille, Fontan Hospital, CURE platform, Lille, France; and Department of Neuroscience (AA) and Department of Biomedical Science of Cells and Systems (IES), University of Groningen, University Medical Center Groningen, Groningen, The Netherlands.

Address correspondence to Simon B. Eickhoff, M.D., at s.eickhoff@fz-juelich.de, or Ji Chen, Ph.D., at jichen.allen@hotmail.com.

Received Jul 8, 2020; revised Sep 10, 2020; accepted Sep 15, 2020.

Supplementary material cited in this article is available online at https://doi.org/10.1016/j.biopsych.2020.09.024.

REFERENCES

1. Kirkpatrick B, Buchanan RW, Ross DE, Ros DE, Carpenter WT Jr (2001): A separate disease within the syndrome of schizophrenia. Arch Gen Psychiatry 58:165–171.
2. Kay SR, Fiszbein A, Opler LA (1987): The Positive and Negative Syndrome Scale (PANSS) for schizophrenia. Schizophr Bull 13:261–276.
3. Lang FU, Walther S, Stegmayer K, Anderson-Schmidt H, Schulze TG, Becker T, Jäger M (2015): Subtyping schizophrenia: A comparison of positive/negative and system-specific approaches. Compr Psychiatry 61:115–121.
4. Pu W, Rolls ET, Guo S, Liu H, Yu Y, Xue Z, *et al.* (2014): Altered functional connectivity links in neuroleptic-naïve and neuroleptic-treated patients with schizophrenia, and their relation to symptoms including volition. Neuroimage Clin 6:463–474.
5. Schilbach L, Derntl B, Aleman A, Caspers S, Clos M, Diederen KMJ, *et al.* (2016): Differential patterns of dysconnectivity in mirror neuron and mentalizing networks in schizophrenia. Schizophr Bull 42:1135–1148.
6. Chen J, Patil KR, Weis S, Sim K, Nickl-Jockschat T, Zhou J, *et al.* (2020): Neurobiological divergence of the positive and negative schizophrenia subtypes identified on a new factor structure of psychopathology using nonnegative factorization: An international machine learning study. Biol Psychiatry 87:282–293.
7. van den Oord EJCG, Rujescu D, Robles JR, Giegling I, Birrell C, Bukszár J, *et al.* (2006): Factor structure and external validity of the PANSS revisited. Schizophr Res 82:213–223.
8. Marder SR, Galderisi S (2017): The current conceptualization of negative symptoms in schizophrenia. World Psychiatry 16:14–24.
9. Stephan KE, Friston KJ, Frith CD (2009): Dysconnection in schizophrenia: From abnormal synaptic plasticity to failures of self-monitoring. Schizophr Bull 35:509–527.
10. Uhlhaas PJ (2013): Dysconnectivity, large-scale networks and neuronal dynamics in schizophrenia. Curr Opin Neurobiol 23:283–290.
11. Pettersson-Yeo W, Allen P, Benetti S, McGuire P, Mechelli A (2011): Dysconnectivity in schizophrenia: Where are we now? Neurosci Biobehav Rev 35:1110–1124.
12. Dong D, Wang Y, Chang X, Luo C, Yao D (2018): Dysfunction of large-scale brain networks in schizophrenia: A meta-analysis of resting-state functional connectivity. Schizophr Bull 44:168–181.
13. Baker JT, Holmes AJ, Masters GA, Yeo BTT, Krienen F, Buckner RL, Öngür D (2014): Disruption of cortical association networks in schizophrenia and psychotic bipolar disorder. JAMA Psychiatry 71:109–118.
14. Baker JT, Dillon DG, Patrick LM, Roffman JL, Brady RO Jr, Pizzagalli DA (2019): Functional connectomics of affective and psychotic pathology. Proc Natl Acad Sci U S A 116:9050–9059.
15. Mwansisya TE, Hu A, Li Y, Chen X, Wu G, Huang X (2017): Task and resting-state fMRI studies in first-episode schizophrenia: A systematic review. Schizophr *Res*189:9–18.
16. Tregellas JR (2014): Neuroimaging biomarkers for early drug development in schizophrenia. Biol Psychiatry 76:111–119.
17. Giraldo-Chica M, Woodward ND (2017): Review of thalamocortical resting-state fMRI studies in schizophrenia. Schizophr Res 180:58–63.
18. Hu ML, Zong XF, Mann JJ, Zheng JJ, Liao YH, Li ZC (2017): A review of the functional and anatomical default mode network in schizophrenia. Neurosci Bull 33:73–84.
19. Mehta UM, Thirthalli J, Aneelraj D, Jadhav P, Gangadhar BN, Keshavanb MS (2014): Mirror neuron dysfunction in schizophrenia and its functional implications: A systematic review. Schizophr Res 160(1–3):9–19.
20. Shen X, Finn ES, Scheinost D, Rosenberg MD, Chun MM, Papademetris X, Constable RT (2017): Using connectome-based predictive modeling to predict individual behavior from brain connectivity. Nat Protoc 12:506–518.
21. Laird AR, Fox PM, Eickhoff SB, Turner JA (2011): Behavioral interpretations of intrinsic connectivity networks. J Cogn Neurosci 23:4022–4037.
22. Laird AR, Eickhoff SB, Li K, Robin DA, Glahn DC, Fox PT (2009): Investigating the functional heterogeneity of the default mode network using coordinate-based meta-analytic modeling. J Neurosci 18:14496–14505.
23. Eickhoff SB, Bzdok D, Laird AR, Kurth F, Fox PT (2012): Activation likelihood estimation revisited. Neuroimage 59:2349–2361.
24. Zilles K, Bacha-Trams M, Palomero-Gallagher N, Amunts K, Friedericic AD (2015): Common molecular basis of the sentence comprehension network revealed by neurotransmitter receptor fingerprints. Cortex 63:79–89.
25. Zilles K, Palomero-Gallagher N, Grefkes C, Scheperjans F, Boy C, Amunts K, Schleicherb A (2002): Architectonics of the human cerebral cortex and transmitter receptor fingerprints: Reconciling functional neuroanatomy and neurochemistry. Eur Neuropsychopharmacol 12:587–599.
26. Richiardi J, Altmann A, Milazzo AC, Chang C, Chakravarty MM, Banaschewski T, *et al.* (2015): Correlated gene expression supports synchronous activity in brain networks. Science 348(6240):1241–1244.
27. Anderson KM, Collins MA, Chin R, Ge T, Rosenberg MD, Holmes AJ (2020): Transcriptional and imaging-genetic association of cortical interneurons, brain function, and schizophrenia risk. Nat Commun 11:1–15.
28. Stagg CJ, Bachtiar V, Amadi U, Gudberg CA, Ilie AS, Sampaio-Baptista C, *et al.* (2014): Local GABA concentration is related to network-level resting functional connectivity. Elife 3:e01465.
29. Kringelbach ML, Cruzat J, Cabral J, Knudsen GM, Carhart-Harris R, Whybrow PC, *et al.* (2020): Dynamic coupling of whole-brain neuronal and neurotransmitter systems. Proc Natl Acad Sci U S A 117:9566–9576.
30. Landek-Salgado MA, Faust TE, Sawa A (2016): Molecular substrates of schizophrenia: Homeostatic signaling to connectivity. Mol Psychiatry 21:10–28.
31. Limongi R, Jeon P, Mackinley M, Das T, Dempster K, Théberge J, *et al.* (2020): Glutamate and dysconnection in the salience network: Neurochemical, effective-connectivity, and computational evidence in schizophrenia. Biol Psychiatry 88:273–281.
32. Howes OD, Kapur S (2009): The dopamine hypothesis of schizophrenia: Version III—the final common pathway. Schizophr Bull 35:549–562.
33. Poels EMP, Kegeles LS, Kantrowitz JT, Slifstein M, Javitt DC, Lieberman JA, *et al.* (2014): Imaging glutamate in schizophrenia: Review of findings and implications for drug discovery. Mol Psychiatry 19:20–29.
34. Selvaraj S, Arnone D, Cappai A, Howes O (2014): Alterations in the serotonin system in schizophrenia: A systematic review and meta-analysis of postmortem and molecular imaging studies. Neurosci Biobehav Rev 45:233–245.
35. Nakazawa K, Zsiros V, Jiang Z, Nakao K, Kolata S, Zhang S, Belforteb JE (2012): GABAergic interneuron origin of schizophrenia pathophysiology. Neuropharmacology 62:1574–1583.
36. Fusar-Poli P, Papanastasiou E, Stahl D, Rocchetti M, Carpenter W, Shergill S, McGuire P (2015): Treatments of negative symptoms in schizophrenia: Meta-analysis of 168 randomized placebo-controlled trials. Schizophr Bull 41:892–899.

37. Miyamoto S, Duncan GE, Marx CE, Lieberman JA (2005): Treatments for schizophrenia: A critical review of pharmacology and mechanisms of action of antipsychotic drugs. Mol Psychiatry 10: 79–104.
38. Tamminga CA, Ivleva EI, Keshavan MS, Pearlson GD, Clementz BA, Witte B, *et al.* (2013): Clinical phenotypes of psychosis in the Bipolar-Schizophrenia Network on Intermediate Phenotypes (B-SNIP). Am J Psychiatry 170:1263–1274.
39. Gardner DM, Murphy AL, O'Donnell H, Centorrino F, Baldessarini RJ (2010): International consensus study of antipsychotic dosing. Am J Psychiatry 167:686–693.
40. Power JD, Barnes KA, Snyder AZ, *et al.* (2012): Spurious but systematic correlations in functional connectivity MRI networks arise from subject motion. Neuroimage 59:2142–2154.
41. Satterthwaite TD, Elliott MA, Gerraty RT, Ruparel K, Loughead J, Calkins ME, *et al.* (2013): An improved framework for confound regression and filtering for control of motion artifact in the preprocessing of resting-state functional connectivity data. Neuroimage 64:240–256.
42. Varikuti DP, Hoffstaedter F, Genon S, Schwender H, Reid AT, Eickhoff SB (2017): Resting-state test-retest reliability of a priori defined canonical networks over different preprocessing steps. Brain Struct Funct 222:1447–1468.
43. Murphy K, Fox MD (2017): Toward a consensus regarding global signal regression for resting state functional connectivity MRI. Neuroimage 154:169–173.
44. Yang GJ, Murray JD, Repovs G, Cole MW, Savic A, Glasser MF, *et al.* (2014): Altered global brain signal in schizophrenia. Proc Natl Acad Sci U S A 111:7438–7443.
45. Tipping ME (2001): Sparse Bayesian learning and the relevance vector machine. J Mach Learn Res 1:211–244.
46. Pervaiz U, Vidaurre D, Woolrich MW, Smith SM (2020): Optimising network modelling methods for fMRI. Neuroimage 211:116604.
47. Dubois J, Galdi P, Paul LK, Adolphs R (2018): A distributed brain network predicts general intelligence from resting-state human neuroimaging data. Philos Trans R Soc Lond B Biol Sci 373:20170284.
48. Snoek L, Miletić S, Scholte HS (2019): How to control for confounds in decoding analyses of neuroimaging data. NeuroImage 184:741–760.
49. More S, Eickhoff SB, Julian C, Patil KR (2020): Confound removal and normalization in practice: A neuroimaging based sex prediction case study. In: Presented at the European Conference on Machine Learning and Principles and Practice of Knowledge Discovery in Databases, September 14–18. Available at: https://bitbucket.org/ghentdatascience/ecmlpkdd20-papers/raw/master/ADS/sub_992.pdf.
50. Combrisson E, Jerbi K (2015): Exceeding chance level by chance: The caveat of theoretical chance levels in brain signal classification and statistical assessment of decoding accuracy. J Neurosci Methods 250:126–136.
51. Meinshausen N, Bühlmann P (2010): Stability selection. J R Stat Soc Ser B Stat Methodol 72:417–473.
52. Dukart J, Holiga Š, Chatham C, Hawkins P, Forsyth A, McMillan R, *et al.* (2018): Cerebral blood flow predicts differential neurotransmitter activity. Sci Rep 8:1–11.
53. Dukart J, Holiga S, Rullmann M, Lanzenberger R, Hawkins PCT, Mehta MA, *et al.* (2020): JuSpace: A tool for spatial correlation analyses of magnetic resonance imaging data with nuclear imaging derived neurotransmitter maps. bioRxiv. https://doi.org/10.1101/2020.04.17.046300.
54. Addington J, Addington D (1999): Neurocognitive and social functioning in schizophrenia. Schizophr Bull 25:173–182.
55. Cohen AS, Forbes CB, Mann MC, Blanchard JJ (2006): Specific cognitive deficits and differential domains of social functioning impairment in schizophrenia. Schizophr Res 81:227–238.
56. Buhle JT, Silvers JA, Wager TD, Lopez R, Onyemekwu C, Kober H, *et al.* (1991): Cognitive reappraisal of emotion: A meta-analysis of human neuroimaging studies. Cereb Cortex 24:2981–2990.
57. Bzdok D, Meyer-Lindenberg A (2018): Machine learning for precision psychiatry: Opportunities and challenges. Biol Psychiatry Cogn Neurosci Neuroimaging 3:223–230.
58. Greene AS, Gao S, Scheinost D, Constable RT (2018): Task-induced brain state manipulation improves prediction of individual traits. Nat Commun 9:1–13.
59. Gao S, Greene AS, Constable RT, Scheinost D (2019): Combining multiple connectomes improves predictive modeling of phenotypic measures. Neuroimage 201:116038.
60. Jiang R, Zuo N, Ford JM, Qi S, Zhi D, Zhuo C, *et al.* (2020): Task-induced brain connectivity promotes the detection of individual differences in brain-behavior relationships. Neuroimage 207:116370.
61. Baron-Cohen S (1995): Mindblindness: An Essay on Autism and Theory of Mind. Cambridge: MIT Press/Bradford, 1–7.
62. Bora E, Pantelis C (2013): Theory of mind impairments in first-episode psychosis, individuals at ultra-high risk for psychosis and in first-degree relatives of schizophrenia: Systematic review and meta-analysis. Schizophr Res 144:31–36.
63. Fretland RA, Andersson S, Sundet K, Andreassen OA, Melle I, Vaskinn A (2015): Theory of mind in schizophrenia: Error types and associations with symptoms. Schizophr Res 162:42–46.
64. Benedetti F, Bernasconi A, Bosia M, Cavallaro R, Dallaspezia S, Falini A, *et al.* (2009): Functional and structural brain correlates of theory of mind and empathy deficits in schizophrenia. Schizophr Res 114:154–160.
65. Das P, Lagopoulos J, Coulston CM, Henderson AF, Malhi GS (2012): Mentalizing impairment in schizophrenia: A functional MRI study. Schizophr Res 134:158–164.
66. Shamay-Tsoory SG, Shur S, Barcai-Goodman L, Medlovich S, Harari H, Levkovitz Y (2007): Dissociation of cognitive from affective components of theory of mind in schizophrenia. Psychiatry Res 149:11–23.
67. Vatansever D, Menon DK, Stamatakis EA (2017): Default mode contributions to automated information processing. Proc Natl Acad Sci U S A 114:12821–12826.
68. Sormaz M, Murphy C, Wang H, Hymers M, Karapanagiotidis T, Poerio G, *et al.* (2018): Default mode network can support the level of detail in experience during active task states. Proc Natl Acad Sci U S A 115:9318–9323.
69. Amft M, Bzdok D, Laird AR, Fox PT, Schilbach L, Eickhoff SB (2015): Definition and characterization of an extended social-affective default network. Brain Struct Funct 220:1031–1049.
70. Silverstein SM, Spaulding WD, Menditto AA, Savitz A, Liberman RP, Berten S, Starobin H (2009): Attention shaping: A reward-based learning method to enhance skills training outcomes in schizophrenia. Schizophr Bull 35:222–232.
71. Schweizer S, Satpute AB, Atzil S, Field AP, Hitchcock C, Black M, *et al.* (2019): The impact of affective information on working memory: A pair of meta-analytic reviews of behavioral and neuroimaging evidence. Psychological Bull 145:566–609.
72. Park S, Gibson C, McMichael T (2006): Socioaffective factors modulate working memory in schizophrenia patients. Neuroscience 139:373–384.
73. Jardri R, Thomas P, Delmaire C, Delion P, Pins D (2013): The neurodynamic organization of modality-dependent hallucinations. Cereb Cortex 23:1108–1117.
74. Whitfield-Gabrieli S, Thermenos HW, Milanovic S, Tsuang MT, Faraone SV, McCarley RW, *et al.* (2009): Hyperactivity and hyperconnectivity of the default network in schizophrenia and in first-degree relatives of persons with schizophrenia. Proc Natl Acad Sci U S A 106:1279–1284.
75. Sinkeviciute I, Begemann M, Prikken M, Oranje B, Johnsen E, Lei WU, *et al.* (2018): Efficacy of different types of cognitive enhancers for patients with schizophrenia: A meta-analysis. NPJ Schizophr 4:22.
76. Stahl SM (2018): Beyond the dopamine hypothesis of schizophrenia to three neural networks of psychosis: Dopamine, serotonin, and glutamate. CNS Spectr 23:187–191.
77. Uno Y, Coyle JT (2019): Glutamate hypothesis in schizophrenia. Psychiatry Clin Neurosci 73:204–215.

78. Abi-Dargham A, Mawlawi O, Lombardo I, Gil R, Martinez D, Huang Y, *et al.* (2002): Prefrontal dopamine D_1 receptors and working memory in schizophrenia. J Neurosci 22:3708–3719.
79. Abi-Dargham A, Xu X, Thompson JL, Gil R, Kegeles LS, Urban N, *et al.* (2012): Increased prefrontal cortical D1 receptors in drug naive patients with schizophrenia: A PET study with [^{11}C] NNC112. J Psychopharmacol 26:794–805.
80. De Rossi P, Chiapponi C, Spalletta G (2015): Brain functional effects of psychopharmacological treatments in schizophrenia: A network-based functional perspective beyond neurotransmitter systems. Curr Neuropharmacol 13:435–444.
81. Lindström LH, Gefvert O, Hagberg G, Lundberg T, Bergström M, Hartvig P, Långström B (1999): Increased dopamine synthesis rate in medial prefrontal cortex and striatum in schizophrenia indicated by L-(β-11C) DOPA and PET. Biol Psychiatry 46:681–688.
82. Elkashef AM, Doudet D, Bryant T, Cohen RM, Li SH, Wyatt RJ (2000): 6-^{18}F-DOPA PET study in patients with schizophrenia. Psychiatry Res 100:1–11.
83. Malhotra AK, Goldman D, Mazzanti C, Clifton A, Breier A, Pickar D (1998): A functional serotonin transporter (5-HTT) polymorphism is associated with psychosis in neuroleptic-free schizophrenics. Mol Psychiatry 3:328–332.
84. Hernandez I, Sokolov BP (1997): Abnormal expression of serotonin transporter mRNA in the frontal and temporal cortex of schizophrenics. Mol Psychiatry 2:57–64.
85. Golimbet VE, Alfimova MV, Shchebatykh TV, Abramova LI, Kaleda VG, Rogaev EI (2004): Serotonin transporter polymorphism and depressive-related symptoms in schizophrenia. Neuropsychiatr Genet 126:1–7.
86. Peitl V, Štefanović M, Karlović D (2017): Depressive symptoms in schizophrenia and dopamine and serotonin gene polymorphisms. Prog Neuropsychopharmacol Biol Psychiatry 77:209–215.
87. Radhakrishnan R, Matuskey D, Nabulsi N, Gaiser E, Gallezot J, Henry S, *et al.* (2020): In vivo 5-HT_6 and 5-HT_{2A} receptor availability in antipsychotic treated schizophrenia patients vs. unmedicated healthy humans measured with [^{11}C] GSK215083 PET. Psychiatry Res Neuroimaging 295:111007.
88. Mauri MC, Paletta S, Maffini M, Colasanti A, Dragogna F, Pace CD, Altamura AC (2014): Clinical pharmacology of atypical antipsychotics: An update. EXCLI J 13:1163–1191.
89. Barkan T, Peled A, Modai I, Weizman A, Rehavi M (2006): Characterization of the serotonin transporter in lymphocytes and platelets of schizophrenia patients treated with atypical or typical antipsychotics compared to healthy individuals. Eur Neuropsychopharmacol 16:429–436.
90. Lian J, Pan B, Deng C (2016): Early antipsychotic exposure affects serotonin and dopamine receptor binding density differently in selected brain loci of male and female juvenile rats. Pharmacol Rep 68:1028–1035.
91. Sahli ZT, Tarazi FI (2018): Pimavanserin: Novel pharmacotherapy for Parkinson's disease psychosis. Expert Opin Drug Discov 13:103–110.
92. Koblan KS, Kent J, Hopkins SC, Krystal JH, Cheng H, Goldman R, Loebel A (2020): A non–D_2-receptor-binding drug for the treatment of schizophrenia. N Engl *J Med* 382:1497–1506.
93. Beaty RE, Rosenberg MD, Benedek M, Chen Q, *et al.* (2018): Robust prediction of individual creative ability from brain functional connectivity. Proc Natl Acad Sci U S A 115:1087–1092.
94. Persson J, Stening E, Nordin K, Söderlund H (2018): Predicting episodic and spatial memory performance from hippocampal resting-state functional connectivity: Evidence for an anterior-posterior division of function. Hippocampus 28:53–66.
95. Hearne LJ, Cocchi L, Zalesky A, Mattingley JB (2017): Reconfiguration of brain network architectures between resting-state and complexity-dependent cognitive reasoning. J Neurosci 37:8399–8411.
96. Cole MW, Bassett DS, Power JD, Braver TS, Petersen SE (2014): Intrinsic and task-evoked network architectures of the human brain. Neuron 83:238–251.
97. Kaminski J, Gleich T, Fukuda Y, Katthagen T, Gallinat J, Heinz A, Schlagenhauf F (2020): Association of cortical glutamate and working memory activation in patients with schizophrenia: A multimodal proton magnetic resonance spectroscopy and functional magnetic resonance imaging study. Biol Psychiatry 87:225–233.